

Unsupervised learning by a nonlinear network with Hebbian excitatory and anti-Hebbian inhibitory neurons

H. Sebastian Seung
Neuroscience Institute and Computer Science Dept.
Princeton University, Princeton, NJ 08544
sseung@princeton.edu

January 1, 2019

Abstract

This paper introduces a rate-based nonlinear neural network in which excitatory (E) neurons receive feedforward excitation from sensory (S) neurons, and inhibit each other through disynaptic pathways mediated by inhibitory (I) interneurons. Correlation-based plasticity of disynaptic inhibition serves to incompletely decorrelate E neuron activity, pushing the E neurons to learn distinct sensory features. The plasticity equations additionally contain “extra” terms fostering competition between excitatory synapses converging onto the same postsynaptic neuron and inhibitory synapses diverging from the same presynaptic neuron. The parameters of competition between $S \rightarrow E$ connections can be adjusted to make learned features look more like “parts” or “wholes.” The parameters of competition between $I - E$ connections can be adjusted to set the typical decorrelatedness and sparsity of E neuron activity. Numerical simulations of unsupervised learning show that relatively few I neurons can be sufficient for achieving good decorrelation, and increasing the number of I neurons makes decorrelation more complete. Excitatory and inhibitory inputs to active E neurons are approximately balanced as a result of learning.

Network models combining Hebbian excitation and anti-Hebbian inhibition have been explored previously by numerous researchers. The model of Földiák [1990] contained neurons that were recurrently connected via all-to-all lateral inhibition, and received feedforward connections from sensory afferents. Anti-Hebbian plasticity of inhibitory connections forced the neurons to decorrelate their activities, thereby enabling the Hebbian feedforward connections to learn distinct sensory features. The term “anti-Hebbian inhibition” was used by Földiák [1990] to mean that correlated activity leads to strengthening of an inhibitory connection (a negative number becomes more negative).

King et al. [2013] studied a model containing excitatory (E) neurons reciprocally connected with inhibitory (I) neurons, and also receiving connections from sensory (S)

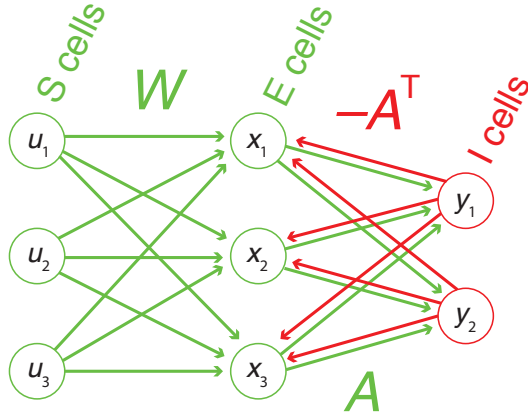


Figure 1: Excitatory-inhibitory net respecting Dale’s Law. The $S \rightarrow E$ connection from u_a to x_i has strength W_{ia} . The E neurons x_i are reciprocally coupled with the I neurons y_α . The $E \rightarrow I$ connection from x_i to y_α has strength $A_{\alpha i}$ and the $I \rightarrow E$ connection from y_α to x_i has strength $-A_{\alpha i}$. The green arrows indicate excitatory connections ($W_{ia} \geq 0$, $A_{\alpha i} \geq 0$), which change via Hebbian plasticity. The red arrows indicate inhibitory connections (note minus sign), which change via anti-Hebbian plasticity. The present model neglects $E \rightarrow E$ and $I \rightarrow I$ connections for simplicity, in order to focus on the computational functions of $I - E$ connections and their plasticity.

afferents (Fig. 1). The $S \rightarrow E$ connections were Hebbian, as in the Földiák [1990] model. The E neurons did not inhibit each other directly, but indirectly through disynaptic $E \rightarrow I \rightarrow E$ pathways mediated by I neurons. This network motif will be called “disynaptic recurrent inhibition,” or just “disynaptic inhibition.” The $E \rightarrow I$ connections were modified by Hebbian plasticity and the $I \rightarrow E$ connections by anti-Hebbian plasticity. King et al. [2013] showed that the I neurons could force the E neurons to decorrelate their activities, enabling Hebbian plasticity of feedforward connections to learn distinct sensory features much as in the original Földiák [1990] model.

This paper introduces a rate-based variant of the King et al. [2013] model, which used spiking integrate-and-fire model neurons for neurobiological realism. A rate-based model is more amenable to mathematical understanding. A rate-based model is also potentially useful for machine learning applications, as it does not require the computational overhead of simulating a spiking network. The novelty of the present model relative to previous rate-based models is that it is (1) nonlinear, and (2) separated into distinct E and I populations that respect Dale’s Law.¹ Some previous rate-based models were nonlinear but did not contain separate E and I populations [Földiák, 1990, Hu

¹Here Dale’s Law means that the outgoing synapses of a neuron are typically either all excitatory or all inhibitory. The original formulation of Dale’s Law is that a neuron secretes a single neurotransmitter at all of its outgoing synapses. The formulations are equivalent if a single neurotransmitter has uniformly excitatory or uniformly inhibitory influences on all postsynaptic neurons. There are known exceptions in which a neuron secretes a single neurotransmitter that excites some postsynaptic neurons and inhibits others, such as photoreceptor synapses onto retinal bipolar cells [Euler et al., 2014], or when a neuron secretes more than one neurotransmitter [Vaaga et al., 2014]. Dale’s Law is also known as Dale’s Principle.

et al., 2014, Pehlevan and Chklovskii, 2014, Seung and Zung, 2017]. Other previous rate-based models had linear neurons that performed principal component analysis, and separated principal neurons and interneurons without respecting Dale’s Law [Plumbley, 1993, Fyfe, 1995, Pehlevan and Chklovskii, 2015].

A first payoff of mathematical tractability is that the plasticity equation for $I - E$ connections can be “derived” from the Földiák [1990] model, or more precisely from the variant due to Seung and Zung [2017]. The derivation results in a Hebbian/anti-Hebbian plasticity equation plus two “extra” terms fostering synaptic competition. Competitive interactions between synapses sharing the same presynaptic or postsynaptic neuron have long been postulated by models of cortical development, and are supported by neurobiological evidence [Miller, 1996]. Surprisingly, the derivation suggests that the parameters of $I - E$ synaptic competition set the typical decorrelatedness and sparseness of E activity.

The derivation regards disynaptic inhibition as an approximate matrix factorization of all-to-all inhibition.² Due to the approximation, decorrelation is expected to be incomplete, with more I neurons leading to more complete decorrelation. Numerical simulations of unsupervised learning from MNIST images of handwritten digits show that good decorrelation is achieved with only a modest number of I neurons, similar to what was already reported by King et al. [2013]. A novelty here is that good decorrelation is achievable (at least in this example) without $I \rightarrow I$ connections, which are lacking in the present model but exist in King et al. [2013].

The mathematical form of competition between $S \rightarrow E$ connections is not fixed by the derivation, and for simplicity is chosen to be the same as for $I - E$ connections. Competition between $S \rightarrow E$ connections determines the sparsity of connectivity, and therefore whether learned features look more like “parts” or “wholes.”

Synaptic competition is linear in the connection strengths; the only nonlinearity is the nonnegativity constraint. This simplicity lends itself to mathematical analysis. The “winners” of synaptic competition are connections to neurons with the most strongly correlated activities; other connections vanish. The number of surviving nonzero connections depends on the numerical parameters of synaptic competition, as well as the values of the activity correlations. Adjusting the parameters makes competition more or less “winner-take-all,” resulting in sparser or fuller connectivity, respectively.

Numerical simulations show that the network exhibits approximate excitatory-inhibitory balance after learning, in the sense that active E cells receive excitatory input that only slightly exceeds inhibitory input. This has an intriguing correspondence with the excitatory-inhibitory balance observed in cortical circuits [Isaacson and Scanziani, 2011]. Previous models of balanced networks have relied upon nonmodifiable random or structured connectivity [Denève and Machens, 2016], rather than connections shaped by plasticity.

²The “derivation” may not really be mathematically justifiable, because it involves approximating a Lagrange multiplier. More precise mathematical justifications are given in a companion paper [Seung, 2018].

1 Network model: description and “derivation”

In the network model, E neurons receive excitatory input from S neurons and inhibit each other through disynaptic pathways mediated by I neurons (Fig. 1). The plasticity equation for $I - E$ connections is “derived” from a previous model in which neurons monosynaptically inhibit each other through all-to-all connections [Földiák, 1990, Seung and Zung, 2017]. In the previous model, anti-Hebbian inhibition served to decorrelate the activity of the neurons. In the present model, anti-Hebbian I neurons serve to *imperfectly* decorrelate the activities of E neurons.

1.1 Disynaptic recurrent inhibition

The network of Fig. 1 has the activity dynamics,

$$x_i := \left[(1 - dt)x_i + dt \lambda_i^{-1} \left(\sum_{a=1}^n W_{ia} u_a - \sum_{\alpha=1}^r y_{\alpha} A_{\alpha i} \right) \right]^+ \quad (1)$$

$$y_{\alpha} = \sum_{i=1}^m A_{\alpha i} x_i \quad (2)$$

Here dt is a step size parameter, which can be set at a small constant value or adjusted adaptively (Appendix A). With the constraint $A_{\alpha i} \geq 0$, the $x \rightarrow y$ connections are excitatory, while the $y \rightarrow x$ connections are inhibitory. The x and y variables are the activities of excitatory (E) and inhibitory (I) neural populations, respectively.³ The u variables are the activities of sensory (S) afferents. The $u \rightarrow x$ connections are also excitatory, $W_{ia} \geq 0$. The numbers of S , E , and I cells are n , m , and r , respectively.

The activation function $[z]^+ = \max\{z, 0\}$ is half-wave rectification. If x_i is initially negative, it becomes nonnegative at the next time step and for all future times, by Eq. (1). A rectification nonlinearity could also be included in Eq. (2), but would have no effect because both A and x are nonnegative.

After the activities converge to a steady state, update the connection matrices via

$$\Delta W_{ia} \propto x_i u_a - \gamma W_{ia} - \kappa \sum_b W_{ib} \quad (3)$$

$$\Delta A_{\alpha j} \propto y_{\alpha} x_j - (q^2 - p^2) A_{\alpha j} - p^2 \sum_i A_{\alpha i} \quad (4)$$

where $\gamma > 0$, $\kappa > 0$, and $q^2 > p^2$. After the updates (3) and (4), any negative elements of W and A are zeroed to maintain nonnegativity.⁴

³The mnemonics eXcitatory and Ynhibitory can be used to remember that E neuron activities are x_i while I neuron activities are y_{α} . Inhibition has infinite speed according to Eq. (2). Inhibition with finite speed could be implemented by some discrete time approximation to $\tau dy_{\alpha}/dt + y_{\alpha} = \sum_i A_{\alpha i} x_i$. For the continuous time case, convergence to a steady state can be proven for sufficiently small τ [Seung et al., 1998]. Similarly, inhibition was faster than excitation in the model of King et al. [2013].

⁴The spiking network model of King et al. [2013] allowed the nonspiking sensory inputs u_a and the $S - E$ connections W_{ia} to have arbitrary signs; the signs are constrained in the present model. The plasticity

The ΔW_{ia} update is said to be Hebbian, because positive correlation between x_i and u_a causes W_{ia} to become more positive. Note that $A_{\alpha j}$ is the strength of the excitatory $x_i \rightarrow y_\alpha$ connection, and $-A_{\alpha j}$ is the strength of the inhibitory $y_\alpha \rightarrow x_i$ connection. The $\Delta A_{\alpha j}$ update is said to be Hebbian when it refers to the excitatory connection, and anti-Hebbian when it refers to the inhibitory connection. The term ‘‘anti-Hebbian’’ is used because positive correlation makes the inhibitory connection more negative.

The connections between E and I neurons are equal and opposite, or antisymmetric. The antisymmetry is a natural outcome of the fact that $E \rightarrow I$ connections are Hebbian while $I \rightarrow E$ connections are anti-Hebbian, so that the same update (4) applies to both. Empirical evidence for approximate antisymmetry of $E \leftrightarrow I$ connections in mouse cortex has been reported by Znamenskiy et al. [2018].

The divisive factor $\lambda_i > 0$ can be interpreted as the inverse slope of the activation function, or a scale factor that divides the connections converging onto the i th E neuron. It is updated via

$$\Delta \lambda_i \propto x_i^2 - q^2 \quad (5)$$

If squared activity x_i^2 is higher than the set point q^2 , then the update increases λ_i , thereby lowering activity in the future. If squared activity x_i^2 is lower than the set point q^2 , then the update decreases λ_i , thereby raising activity in the future. Therefore Eq. (5) amounts to homeostatic regulation of activity so that $\langle x_i^2 \rangle \approx q^2$.

1.2 ‘‘Derivation’’ of $I - E$ plasticity equation

Eqs. (1) and (2) can be combined into the dynamics

$$x_i := \left[(1 - dt)x_i + dt \lambda_i^{-1} \left(\sum_a W_{ia} u_a - \sum_j (A^\top A)_{ij} x_j \right) \right]^+ \quad (6)$$

This equation has all-to-all inhibitory connections between the x neurons (which are now inhibitory rather than excitatory). Combined with the plasticity equations (3)-(5), Eq. (6) resembles a variant of the Földiák [1990] model due to Seung and Zung [2017]. The dynamics of activity in the previous model were⁵

$$x_i := \left[(1 - dt)x_i + dt L_{ii}^{-1} \left(\sum_a W_{ia} u_a - \sum_{j, j \neq i} L_{ij} x_j \right) \right]^+ \quad (7)$$

equation for W_{ia} was Hebbian plus weight decay of the form proposed by Oja [1982]. For other classes of connections, King et al. [2013] introduced a ‘‘Correlation Measuring’’ rule, which was designed to make connection strength proportional to the covariance of presynaptic and postsynaptic activity at the stationary state of learning. The activities of both E and I neurons were regulated by a homeostatic rule; in the present model only the E activities are regulated. King et al. [2013] used the homeostatic rule of Földiák [1990] rather than Eq. (5) which was also used by Seung and Zung [2017]. King et al. [2013] included $I \rightarrow I$ connections whereas the present model omits them.

⁵A subtlety is that the diagonal term $(A^\top A)_{ii}$ does not vanish, so that Eqs. (6) and (7) are not exactly equivalent. However, one can show that the Lyapunov functions of the activity dynamics are equivalent with the identification $L = \Lambda + A^\top A$.

The elements of the matrix L were updated via⁶

$$\Delta L_{ij} \propto x_i x_j - D_{ij} \quad (8)$$

where

$$D_{ij} = \begin{cases} p^2, & i \neq j, \\ q^2, & i = j \end{cases} \quad (9)$$

Seung and Zung [2017] showed formally that L is a Lagrange multiplier that enforces the constraint $\langle x_i x_j \rangle \leq D_{ij}$, where $\langle \rangle$ denotes an average over stimuli, and that Eq. (8) can be viewed as a gradient update $\Delta L_{ij} \propto \partial S / \partial L_{ij}$ for some function S .

Now consider the parametrization $L = \Lambda + A^\top A$, meaning that $L - \Lambda$ has a factorized form. Then a gradient update for A follows from naive application of the chain rule,

$$\Delta A_{\alpha j} \propto \frac{\partial S}{\partial A_{\alpha j}} = \sum_i A_{\alpha i} \frac{\partial S}{\partial L_{ij}} = \sum_i A_{\alpha i} (x_i x_j - D_{ij}) \quad (10)$$

Eq. (4) follows from Eqs. (9) and (10). A gradient update for the diagonal matrix Λ similarly leads to Eq. (5).

The preceding “derivation” regards the disynaptic inhibition of the current model as an approximation to all-to-all inhibition. The approximation has low rank if I neurons are less numerous than E neurons. “Derivation” is in quotes because the parametrized form for a Lagrange multiplier may not really be justifiable. Alternative mathematical interpretations of the model are given in a companion paper [Seung, 2018].

To summarize, the role of the plasticity equation (4) is to approximately enforce the constraint $\langle x_i x_j \rangle \leq D_{ij}$, or incompletely decorrelate E neuron activity. Decorrelation is expected to become more complete with increasing number of I neurons, because the approximation $L = \Lambda + A^\top A$ should improve as the rank of A increases. In the following, completeness of decorrelation will be assessed using numerical simulations.

2 Numerical demonstration of decorrelation

Numerical simulations of the network were done for sensory stimuli drawn from the MNIST images of handwritten digits. The images were normalized so that the minimum and maximum pixel values were 0 and 1, respectively. The network saw each of the 60,000 training images once during learning.

The network contained 784 S neurons, 64 E neurons and 5 I neurons. The elements of W were drawn from a uniform distribution, and normalized so that $\sum_a W_{ia} = 1$ for all i . The elements of A were drawn from a uniform distribution on the interval $[0, 0.1]$. The λ_i were initialized at unity. The learning rate parameters were 0.1 for A and Λ and 0.001 for W . After each λ_i update via Eq. (5), a bound constraint $\lambda \geq \lambda_{min}$ was applied

⁶For $i \neq j$, Eq. (8) is exactly as in Földiák [1990]. For $i = j$, Eq. (8) is based on x_i^2 and divisively modifies Eq. (7) while the analogous equation in Földiák [1990] is based on x_i and subtractively modifies the neural network dynamics.

with $\lambda_{min} = 0.01$. This is not always necessary, but is helpful for avoiding numerical instability in some cases.

The base parameter configuration used $\gamma/\kappa = 5$ (specifically $\kappa = 0.01$, $\gamma = 0.05$) as the synaptic competition parameters in the W update (3) and $p/q = 1/3$ (specifically $p = 0.03$, $q = 0.09$) in the A update (4). Other parameter configurations differed by altering one parameter of the base configuration, so that $\gamma = 0.5$ (Fig. 2), $p = 0.06$ (Figs. 3, 4, 5, 8), or $r = 1, 10$ (Fig. 6). Note that the learned representations (up to trivial rescalings) depend on κ , γ , p , and q only through the ratios κ/γ and p/q .⁷

2.1 The E neurons learn sensory features

For each of the 64 E neurons, the set of convergent $S \rightarrow E$ connections can be viewed as an image (Fig. 2). The images will be called “sensory features,” or simply “features.” For the base parameter configuration ($\gamma/\kappa = 5$), the features are more sparse and resemble character “strokes.” For $\gamma/\kappa = 50$, the features are more full, and look almost like entire digits. By controlling sparsity of $S \rightarrow E$ connections, the ratio γ/κ effectively determines whether E neurons learn “parts” or “wholes.”

2.2 E neurons are more selective than I neurons

At the beginning of learning, all E neurons are active when the network dynamics (1) converges to a steady state. As learning proceeds, some neurons become inactive at the steady state (Fig. 3). Once learning has converged, E activity is sparse at the steady state, while all I neurons are active for all stimuli (Fig. 4). The activity of E neurons is more sparse for smaller values of p/q (Figs. 3 and 4).

This behavior can be understood from the idea, introduced in Section 1.2, that anti-Hebbian inhibition enforces the constraint $\langle x_i x_j \rangle \leq D_{ij}$. If equality holds for $i = j$, the constraint takes the form

$$\frac{\langle x_i x_j \rangle}{\sqrt{\langle x_i^2 \rangle \langle x_j^2 \rangle}} \leq \frac{p^2}{q^2}, \quad (11)$$

where the left hand side is the cosine similarity of the activities of E neurons i and j . In other words, anti-Hebbian inhibition encourages the activities of E neurons to be dissimilar or decorrelated if p/q is small (Fig. 5). Because the activities are nonnegative, decorrelation leads to sparsity.

2.3 Decorrelation is incomplete

By the arguments of Section 1.2, we expect that decorrelation should be less complete when I cells are less numerous. Indeed, reducing to a single I neuron results in a long tail of highly correlated E cell pairs (Fig. 6). The tail is reduced in the base parameter

⁷Transforming a steady state of learning by doubling W and Λ , scaling A and y by $\sqrt{2}$, and holding x fixed is a steady state of learning for κ and γ halved. Transforming a steady state of learning by doubling x , y , and W while holding A and Λ fixed yields a steady state of learning for p and q doubled. This can be verified in an average velocity approximation, according to which a steady state of learning satisfies $\langle \Delta W_{ia} \rangle = 0$ and $\langle \Delta A_{ai} \rangle = 0$.

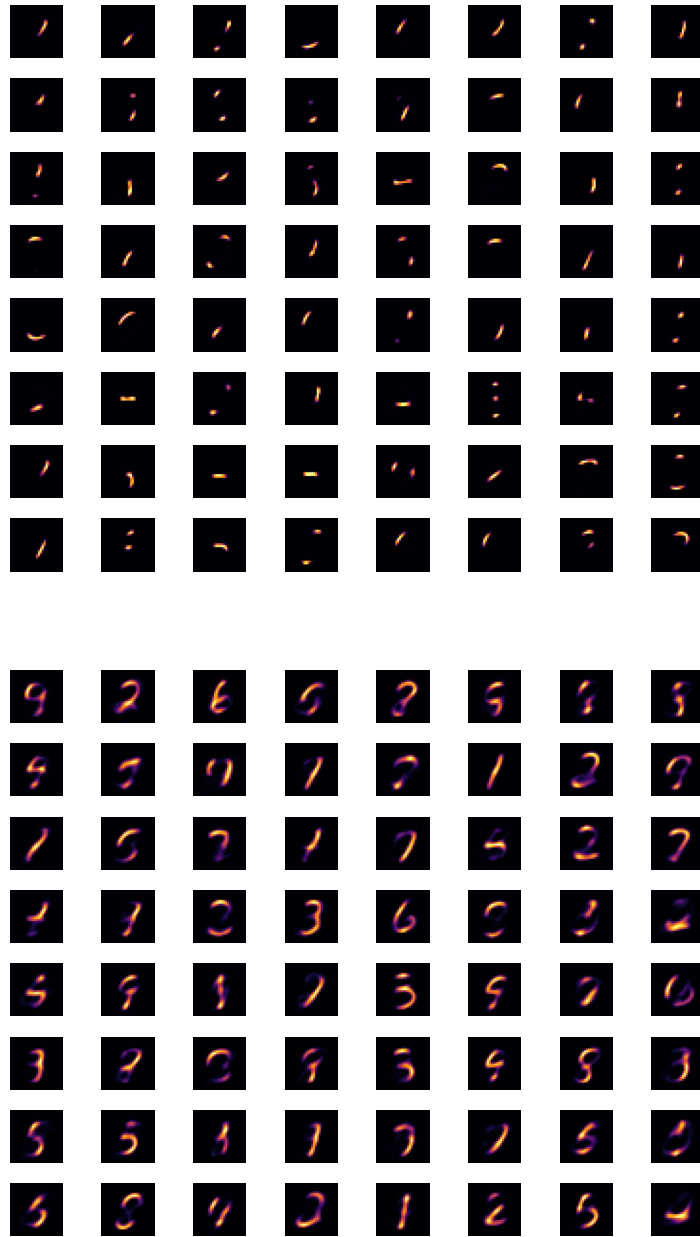


Figure 2: For each E neuron, the convergent $S \rightarrow E$ connections constitute a sensory feature learned from the stimuli. (a) Learned features for $\gamma/\kappa = 5$ are more sparse, resembling character “strokes.” (b) Learned features for $\gamma/\kappa = 50$ are more full, looking almost like entire digits.

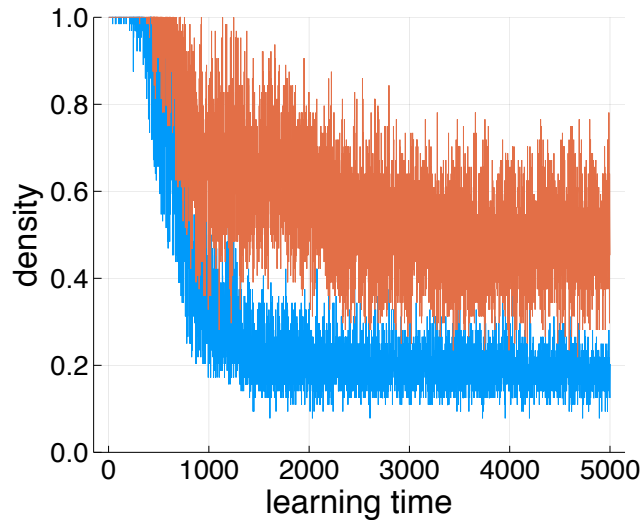


Figure 3: *E* neuron activity starts out full, and sparsens as learning proceeds. Activity ends up sparser for $p/q = 1/3$ (blue) than for $p/q = 2/3$ (red).

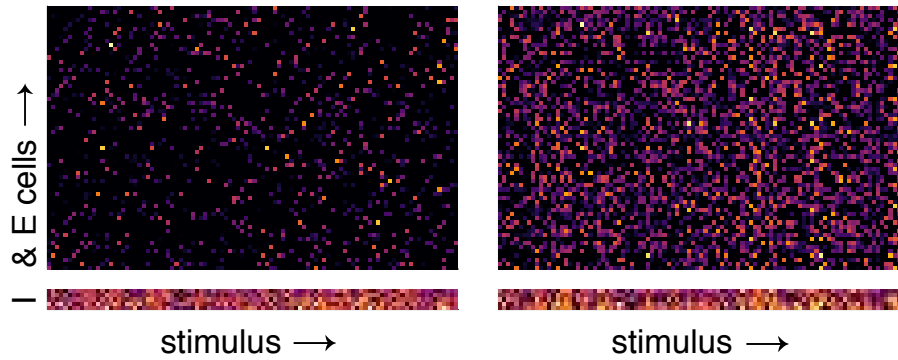


Figure 4: *E* cells (top) are more sparsely active than *I* cells (bottom), which are fully active. *E* cell activity is more sparse for $p/q = 1/3$ (left) and more full for $p/q = 2/3$ (right).

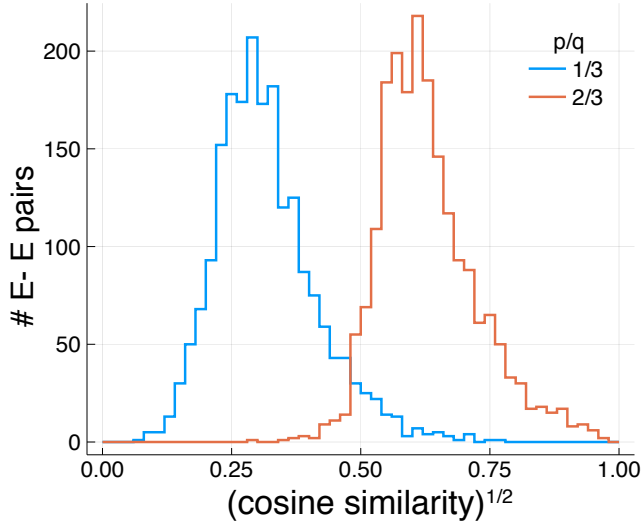


Figure 5: The ratio p/q controls the degree of decorrelation. Histograms of the square root of the cosine similarity of $E - E$ pairs for $p/q = 1/3$ (blue) and $p/q = 2/3$ (red). The histograms are peaked near p/q , roughly in accord with Eq. (11).

configuration of 5 I neurons, and further reduced when the number of I neurons is increased to 10 (Fig. 6).⁸

3 Synaptic competition

The first terms of the plasticity equations (3) and (4) are nonnegative, since all neural activities are nonnegative. Therefore the connection strengths could increase without bound, were it not for the “extra” terms in the plasticity equations. In the plasticity equation (3) for ΔW_{ia} , the “weight decay” term $-\gamma W_{ia}$ is said to be homosynaptic, since the change in the connection depends on the strength of the same connection. The other term $-\kappa \sum_b W_{ib}$ is heterosynaptic, since through it ΔW_{ia} depends on all other connections converging onto the i th E cell.⁹

The roles of the two terms can be explained with a financial analogy. The weight decay term $-\gamma W_{ia}$ is larger for stronger connections, and therefore acts like a “flat tax.” The heterosynaptic term $-\kappa \sum_a W_{ia}$ is the same for all connections, large or small, converging onto neuron i . This amounts to a “regressive tax” on convergent connections. By itself the regressive tax would lead to “winner-take-all”: all connections would

⁸One might expect that complete decorrelation is guaranteed at $r = n$ (full rank). However this is not necessarily true as A is constrained to be nonnegative.

⁹In models of cortical development, it is more common to constrain the sums in Eqs. (3) and (4), so that for example $\sum_b W_{ib} = \rho$ [Von der Malsburg, 1973, Miller and MacKay, 1994]. This has the biological interpretation that the synapses are competing for fixed amount of resources. The constraint can be implemented in a “soft” way by substituting $\sum_b W_{ib} - \rho$ for $\sum_b W_{ib}$ in Eq. (3), as was done by Seung and Zung [2017]. Here the constraint is eliminated altogether to reduce the number of parameters and simplify the model.

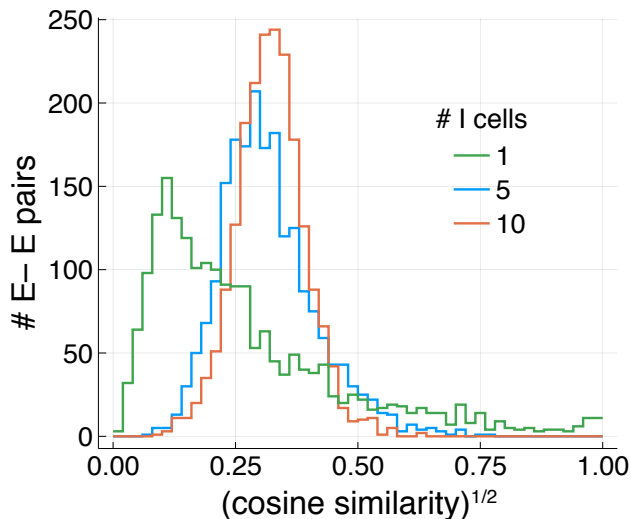


Figure 6: Decorrelation of E neuron activity becomes more complete with more I neurons. Histograms are of the square root of cosine similarity with $p/q = 1/3$. For a single I neuron (green), the histogram peaks well below p/q , and has a long tail to the right. For 5 I neurons (blue), the histogram is peaked near p/q and the tail to the right is reduced. For 10 I neurons (red) the tail to the right is further reduced.

vanish except for a single winner. The flat tax is more egalitarian: adding it prevents a single winner from dominating.

An analogous combination of homosynaptic and heterosynaptic terms is also found in the plasticity equation (4) for $\Delta A_{\alpha i}$. In this case the heterosynaptic term fosters competition between inhibitory connections diverging from the α th I neuron and excitatory connections converging onto the α th I neuron.

Competition between synapses is simple enough for analytical treatment. Eq. (4) and nonnegativity of A imply that

$$(q^2 - p^2) A_{\alpha j} \approx \left[\langle y_{\alpha} x_j \rangle - p^2 \sum_i A_{\alpha i} \right]^+ \quad (12)$$

at a stationary state of learning. Numerical simulations (Fig. 7) agree well with Eq. (12). For each I neuron α , the top k connections are linearly related to the top k correlations, while the rest of the connections vanish. The number k of surviving connections varies from neuron to neuron. It depends on the ratio p/q as well as the values of the activity correlations through inequalities derived in Appendix B. Simple statements can be made for limiting cases of p/q . The competition is “winner-take-all” as $p/q \rightarrow 1$, with a single nonzero connection surviving for each I neuron. As $p/q \rightarrow 0$, on the other hand, all connections survive.

Visualization of the $E - I$ connections from numerical simulations (Fig. 8) illustrates that a fuller A matrix corresponds to sparser E activity. Small p/q means weaker competition and less sparse A connections. At the same time, it means sparser and

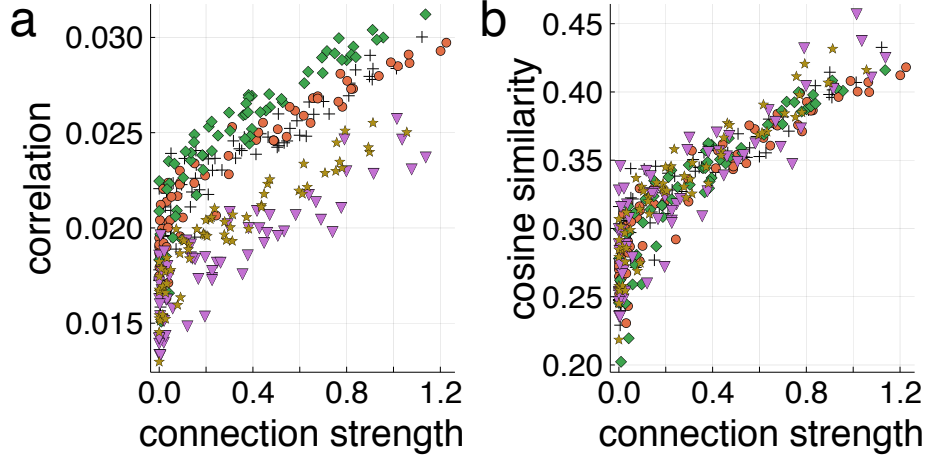


Figure 7: $I - E$ connection strength is linearly related to correlation or response similarity. The connections of each I neuron are distinguished by color and marker type. (a) Correlation $\langle y_\alpha x_i \rangle$ versus connection strength $A_{\alpha i}$ has the same slope but different intercept for each I neuron, consistent with Eq. (12). (b) The relation of cosine similarity to connection strength varies less across I neurons.

more decorrelated E activity, by Eq. (11).

The $S \rightarrow E$ connections can be analyzed similarly. Equation (3) and nonnegativity of W imply that

$$\gamma W_{ia} = \left[\langle x_i u_a \rangle - \kappa \sum_b W_{ib} \right]^+ \quad (13)$$

at a stationary state of learning. Numerical simulations (Fig. 9) agree well with Eq. (13). For each E neuron i , the top k connections are linearly related to the top k correlations, while the rest of the connections vanish. The number k of surviving connections varies from neuron to neuron, and is governed by an inequality derived in Appendix B.

4 Excitatory-inhibitory balance

At a steady state of the activity dynamics, Eq. (1) implies that

$$x_i = \left[\lambda_i^{-1} \left(\sum_{a=1}^m W_{ia} u_a - \sum_{\alpha=1}^r y_\alpha A_{\alpha i} \right) \right]^+$$

The activity of the i th E cell is determined by the difference between its excitatory input $\lambda_i^{-1} \sum_a W_{ia} u_a$ (due to $S \rightarrow E$ connections) and its inhibitory input $\lambda_i^{-1} \sum_\alpha y_\alpha A_{\alpha i}$ (due to $I \rightarrow E$ connections). Active E cells are those for which excitatory input exceeds inhibitory input. Numerical simulations show that excitatory input only slightly exceeds inhibitory input for active cells (Fig. 10). This is reminiscent of a phenomenon reported for cortical neurons and known as excitatory-inhibitory balance [Isaacson and

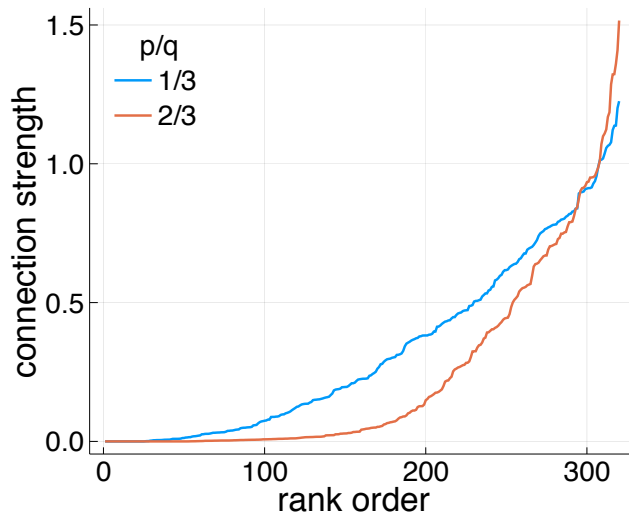


Figure 8: Sparser E activity corresponds with a fuller A matrix. The elements of A are graphed after sorting in increasing order. The matrix is fuller for $p/q = 1/3$ than for $p/q = 2/3$. Activity of E neurons is sparser and more decorrelated for $p/q = 1/3$, as was shown by Figs. (4) and (5).

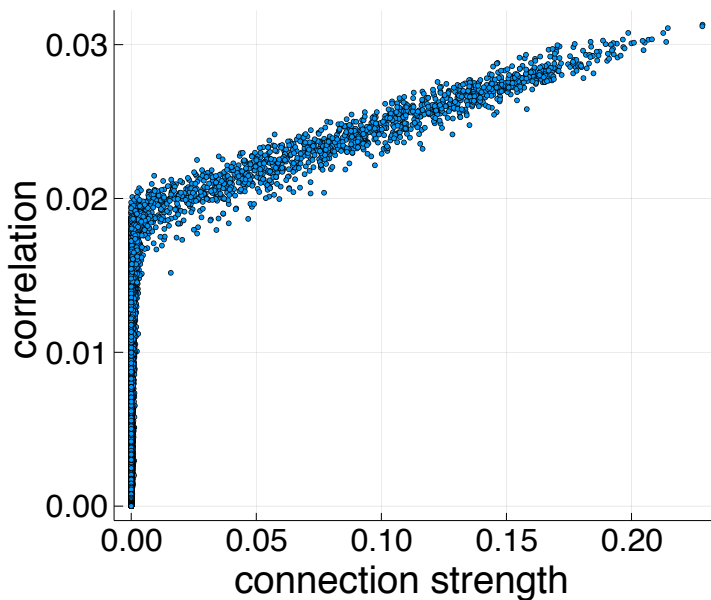


Figure 9: $S \rightarrow E$ connection strength is linearly related to correlation. Correlation $\langle x_i u_a \rangle$ versus connection strength W_{ia} has the same slope and intercept for every E neuron, consistent with Eq. (13) and the fact that $\sum_b W_{ib}$ turns out to vary little across i .

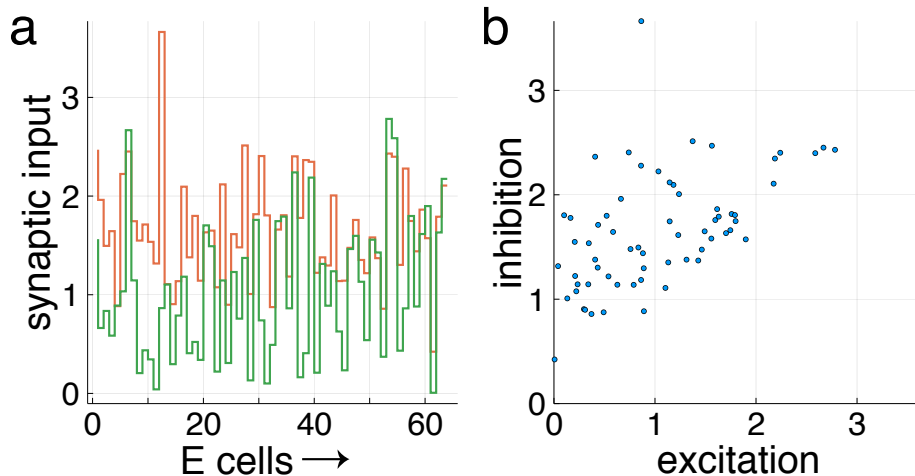


Figure 10: Excitatory-inhibitory balance as a byproduct of learning via Hebbian excitation and anti-Hebbian inhibition. (a) Excitatory input $\lambda_i^{-1} \sum_a W_{ia} u_a$ (green) and inhibitory input $\lambda_i^{-1} \sum_a \gamma_a A_{ai}$ (red) to each E cell i for a single stimulus after convergence of the activity dynamics. Only a few E cells are active, those for which excitation (green) exceeds inhibition (red). (b) Excitation only slightly exceeds inhibition for active cells. Active E cells correspond to points below the main diagonal (excitation equals inhibition), and these points are only slightly below.

Scanziani, 2011]. Previous computational models of balanced networks have focused on explaining Poisson-like variability of spiking activity [Denève and Machens, 2016]. The current network is not intended as an explanation of spiking variability, as it is a rate-based model. The novelty is that excitatory-inhibitory balance emerges from synaptic plasticity rather than the nonmodifiable random or structured connectivity of previous models [Denève and Machens, 2016].

5 Discussion

Numerical simulations have shown that a modest number of I neurons can be sufficient to decorrelate the activities of E neurons, consistent with the fact that inhibitory neurons are a small minority of cortical neurons. Rather complete decorrelation is achievable without $I-I$ connections. Including $I-I$ connections, as in the prior spiking network model of King et al. [2013], would add more neurobiological realism as well as computational power. Future work will consider the computational roles of $E-E$ as well as $I-I$ connections.

Many classes of inhibitory neurons are known to exist in the cortex. King et al. [2013] proposed that the anti-Hebbian I neurons in their model should be identified with parvalbumin-positive fast-spiking basket cells, which are fast, have high average firing rates, are reciprocally coupled with excitatory cells, and exhibit plasticity. This class of cells is also a reasonable candidate for the I neurons in the present model.

The number of connections in a network with disynaptic inhibition is much reduced relative to a network with all-to-all inhibition. Therefore disynaptic inhibition can be regarded as a more efficient way of achieving decorrelation. In this view, incompleteness of decorrelation is something to be eliminated or reduced as much as possible. Alternatively, one can imagine that incompleteness of decorrelation could have an important computational function. Perhaps the remaining correlations in the output of the network could serve as a basis for further learning by another network.

Acknowledgments

The author is grateful for helpful discussions with C. Pehlevan and D. Chklovskii. The research is supported in part by the Intelligence Advanced Research Projects Activity (IARPA) via DoI/IBC contract number D16PC0005, and by the National Institutes of Health via U19 NS104648 and U01 NS090562.

A Optimization by the gradient projection algorithm

Eq. (1) is a diagonally rescaled gradient projection algorithm,

$$\begin{aligned}\mathbf{x} &:= [(1 - dt)\mathbf{x} - dt\Lambda^{-1}\partial L/\partial\mathbf{x}]^+ \\ &:= [(1 - dt)\mathbf{x} + dt\Lambda^{-1}(W\mathbf{u} - A^\top A\mathbf{x})]^+\end{aligned}\tag{14}$$

for solving the optimization problem

$$\min_{\mathbf{x} \geq 0} L(\mathbf{x})\tag{15}$$

where

$$\begin{aligned}L(\mathbf{x}) &= \frac{1}{2}\mathbf{x}^\top (\Lambda + A^\top A)\mathbf{x} - \mathbf{x}^\top W\mathbf{u} \\ &= \frac{1}{2}\sum_i \lambda_i x_i^2 + \frac{1}{2}\sum_\alpha \left(\sum_i A_{\alpha i} x_i\right)^2 - \sum_{ia} W_{ia} x_i u_a\end{aligned}\tag{16}$$

A simple backtracking line search was found to be more efficient than a fixed value of dt . Namely, if a gradient projection step causes L to increase, then the step is rejected and the step size parameter dt is halved. If L does not increase, the step is accepted, and dt is increased by 1 percent with a ceiling of 0.5. The iteration terminates when the root mean square of $\partial L/\partial x_i$ for i such that $x_i > 0$ is less than 10^{-3} . For each stimulus, dt is initialized at 0.4.

B Number of surviving connections

B.1 Disynaptic inhibition

Without loss of generality, assume that $\langle y_{\alpha x_1} \rangle \geq \langle y_{\alpha x_2} \rangle \geq \dots \geq \langle y_{\alpha x_n} \rangle$. Then we have $A_{\alpha 1}, \dots, A_{\alpha k} > 0$ and $A_{\alpha, k+1} = \dots = A_{\alpha n} = 0$ for k satisfying

$$\langle y_{\alpha x_{k+1}} \rangle \leq p^2 \sum_{i=1}^k A_{\alpha i} < \langle y_{\alpha x_k} \rangle$$

Summing Eq. (12) over $j = 1, \dots, k$ yields

$$(q^2 - p^2) \sum_{j=1}^k A_{\alpha j} = \sum_{j=1}^k \langle y_{\alpha x_j} \rangle - p^2 k \sum_{i=1}^k A_{\alpha i}$$

from which it follows that

$$\sum_{j=1}^k A_{\alpha j} = \frac{1}{q^2 + (k-1)p^2} \sum_{j=1}^k \langle y_{\alpha x_j} \rangle$$

Substituting back into the first inequality yields

$$\langle y_{\alpha x_{k+1}} \rangle \leq \frac{p^2}{q^2 + (k-1)p^2} \sum_{j=1}^k \langle y_{\alpha x_j} \rangle < \langle y_{\alpha x_k} \rangle$$

Note that this condition depends on p and q only through their ratio p/q . If correlations are held fixed, the competition is “winner-take-all” ($k = 1$) as $p/q \rightarrow 1$, with only one nonzero connection surviving. The condition for all connections to survive is

$$\frac{\sum_{j=1}^n \langle y_{\alpha x_j} \rangle}{\langle y_{\alpha x_n} \rangle} \leq \frac{q^2 + (n-1)p^2}{p^2}$$

which is satisfied as $p/q \rightarrow 0$ if correlations are held fixed.

B.2 Feedforward excitation

Without loss of generality, assume that $\langle x_i u_1 \rangle \geq \langle x_i u_2 \rangle \geq \dots \geq \langle x_i u_m \rangle$. Then we have $W_{i1}, \dots, W_{ik} > 0$ and $W_{i, k+1} = \dots = W_{im} = 0$ for k satisfying

$$\langle x_i u_{k+1} \rangle \leq \frac{1}{\gamma/\kappa + k} \sum_{a=1}^k \langle x_i u_a \rangle < \langle x_i u_k \rangle$$

The competition is winner-take-all as $\gamma/\kappa \rightarrow 0$.

References

- Sophie Denève and Christian K Machens. Efficient codes and balanced networks. *Nature neuroscience*, 19(3):375, 2016.
- Thomas Euler, Silke Haverkamp, Timm Schubert, and Tom Baden. Retinal bipolar cells: elementary building blocks of vision. *Nature Reviews Neuroscience*, 15(8):507–519, 2014.
- Peter Földiák. Forming sparse representations by local anti-hebbian learning. *Biological cybernetics*, 64(2):165–170, 1990.
- Colin Fyfe. Introducing asymmetry into interneuron learning. *Neural Computation*, 7(6):1191–1205, 1995.
- Tao Hu, Cengiz Pehlevan, and Dmitri B Chklovskii. A hebbian/anti-hebbian network for online sparse dictionary learning derived from symmetric matrix factorization. In *Signals, Systems and Computers, 2014 48th Asilomar Conference on*, pages 613–619. IEEE, 2014.
- Jeffrey S Isaacson and Massimo Scanziani. How inhibition shapes cortical activity. *Neuron*, 72(2):231–243, 2011.
- Paul D King, Joel Zylberberg, and Michael R DeWeese. Inhibitory interneurons decorrelate excitatory cells to drive sparse code formation in a spiking model of v1. *The Journal of Neuroscience*, 33(13):5475–5485, 2013.
- Kenneth D Miller. Synaptic economics: competition and cooperation in synaptic plasticity. *Neuron*, 17(3):371–374, 1996.
- Kenneth D Miller and David JC MacKay. The role of constraints in hebbian learning. *Neural Computation*, 6(1):100–126, 1994.
- Erkki Oja. Simplified neuron model as a principal component analyzer. *Journal of mathematical biology*, 15(3):267–273, 1982.
- Cengiz Pehlevan and Dmitri Chklovskii. A normative theory of adaptive dimensionality reduction in neural networks. In *Advances in neural information processing systems*, pages 2269–2277, 2015.
- Cengiz Pehlevan and Dmitri B Chklovskii. A hebbian/anti-hebbian network derived from online non-negative matrix factorization can cluster and discover sparse features. In *Signals, Systems and Computers, 2014 48th Asilomar Conference on*, pages 769–775. IEEE, 2014.
- Mark D Plumbley. Efficient information transfer and anti-hebbian neural networks. *Neural Networks*, 6(6):823–833, 1993.
- H Sebastian Seung. Two correlation games for a nonlinear network with hebbian excitatory and anti-hebbian inhibitory neurons. *arXiv*, 2018.

- H Sebastian Seung and Jonathan Zung. A correlation game for unsupervised learning yields computational interpretations of hebbian excitation, anti-hebbian inhibition, and synapse elimination. *arXiv preprint arXiv:1704.00646*, 2017.
- H Sebastian Seung, Tom J Richardson, Jeffrey C Lagarias, and John J Hopfield. Minimax and hamiltonian dynamics of excitatory-inhibitory networks. In *Advances in neural information processing systems*, pages 329–335, 1998.
- Christopher E Vaaga, Maria Borisovska, and Gary L Westbrook. Dual-transmitter neurons: functional implications of co-release and co-transmission. *Current opinion in neurobiology*, 29:25–32, 2014.
- Chr Von der Malsburg. Self-organization of orientation sensitive cells in the striate cortex. *Kybernetik*, 14(2):85–100, 1973.
- Petr Znamenskiy, Mean-Hwan Kim, Dylan R Muir, Maria Florencia Iacaruso, Sonja B Hofer, and Thomas D Mrsic-Flogel. Functional selectivity and specific connectivity of inhibitory neurons in primary visual cortex. *bioRxiv*, page 294835, 2018.